Mechatronic Approach towards Lightweight Mirrors with Active Optics for Telescope Systems ⋆

Christian Schwaer *, **Andreas Sinn** *, **Georg Schitter** *

* *Automation and Control Institute (ACIN), TU Wien, Gußhausstraße 27-29, 1040 Vienna, Austria, (e-mail: schwaer@acin.tuwien.ac.at)*

Abstract: Midsized telescopes receive currently a lot of interest due to their application in free space optical (FSO) communication and space debris observation. This paper analyzes an active mirror support system of a very thin meniscus with a diameter of 1 m and 25 mm thickness for the application in a lightweight, low-cost telescope. An analytic model for self-weight surface deflection is used to determine the number of concentric continuous support rings and optimize their radii to sufficiently support the mirror. The obtained radii are used as initial value for a finite element analysis (FEA) to include shear effects and the presence of a central hole for optical access, enabling further optimization. Following that, a transition from continuous support rings to point supports is made. With a number of 24 support points, a surface RMS error of 10.9 nm can be achieved. Additionally, the requirements for an active support to correct low order aberrations are determined.

Keywords: Active Optics, Meniscus Mirror, System Analysis, Optimization, Optomechatronics.

1. INTRODUCTION

Currently, medium-sized telescopes in the range of 0.3 m to 1.5 m are obtaining increasing importance in several applications. One important application is the utilization as optical ground station (OGS) in free space optical (FSO) communication which offers great benefits compared to conventional radio frequency communication, such as large data rate, less power consumption, low mass requirement, high security and license free spectrum [Kaushal and Kaddoum (2015)]. Especially for uplinks/downlinks to satellites, FSO communication has advantages of low terminal size and weight at the satellite, smaller aperture sizes and low power consumption [Leitgeb et al. (2009)]. For communication to satellites in deep space or observations and tracking of space debris (SD) through reflected sunlight, telescopes with large light-gathering power are needed [Hemmati et al. (2006)].
First satellite-to-ground links have been established in 2001 using the 1 m European Space Agency's OGS at the Teide Observatory on Tenerife [Garcia-Talavera et al. (2002)]. The NASA Jet Propulsion Laboratory's (JPL) Optical Communications Telescope Laboratory (OCTL) also uses a 1 m telescope for FSO communication [Kovalik et al. (2014)]. The IN-orbit and Networked Optical Ground Stations Experimental Verification Advanced Testbed (INNOVA) operated by the National Institute of Information and Communications Technology (NICT) consists of four OGSs, three with 1 m and one with 1.5 m [Toyoshima et al. (2013)]. For SD research, NASA uses the Meter-Class Autonomous Telescope (MCAT) with 1.3 m.

⋆ This work was funded by the Austrian research funding association (FFG) under the scope of the Austrian Space Applications Program (854050)

These ground stations are often co-located with astronomical observatories, i.e. with existing infrastructure, and are fixed in their location, partly because of their large mass. For instance, the 1 m OGS of NICT has a total mass of 7500 kg [Toyoshima and Carrasco-Casado (2016)]. However, telescopes at fixed locations have a high chance that local weather effects such as fog, rain and clouds between the telescope and a satellite or SD degrade the system performance and can even lead to inability to use the system [Khalighi and Uysal (2014), Link et al. (2005), Wojcik et al. (2005)]. Additionally, Schulz et al. (2012) estimated the initial investment costs of a 40 cm telescope for communication with LEO satellites to be between 1,4 and 3,4 million Euro. If telescopes can be built much lighter to relocate them easily to avoid seasonal weather or target individual satellite orbits and if the cost of ground stations and supporting infrastructure can be significantly reduced, the problem of ground station availability can be alleviated [Riesing (2018)].
To build lighter and less expensive OGSs, telescopes with smaller aperture for FSO communication have been developed in recent years. The DLR developed the Transportable Optical Ground Station (TOGS) with 60 cm in diameter [Shrestha and Brechtelsbauer (2012)], as well as the Transportable Adaptive Optical Ground Station (TAOGS) with a diameter of 27 cm and implemented adaptive optics to mitigate the influences of atmospheric distortions [Saucke et al. (2016)]. The portable 30 cm telescope (PorTel) can be carried by a single person and makes use of commercial-off-the-shelf (COTS) parts to drastically reduce the costs [Riesing et al. (2017)]. These telescopes can be arranged in an array to achieve the same size aperture with greater flexibility and lower cost [Boroson et al. (2004), Kudielka et al. (1996)]. However, they require additional hardware for delay compensation, array

Pre-print version of the article: C. Schwaer, A. Sinn, and G. Schitter, "Mechatronic Approach towards Lightweight Mirrors with Active Optics for Telescope Systems", *8th IFAC Symposium on Mechatronic Systems MECHATRONICS 2019*, 2019.
DOI: 10.1016/j.ifacol.2019.11.641

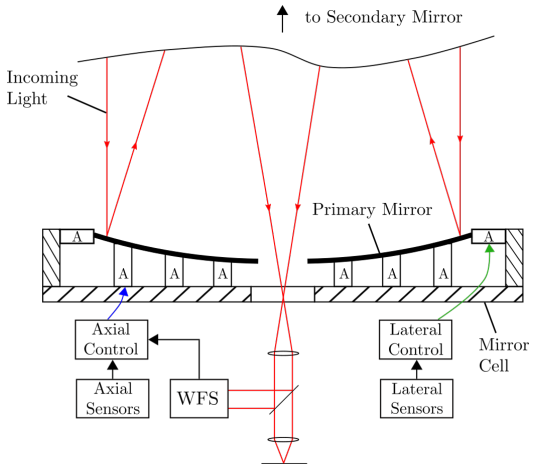

Fig. 1. Layout of the primary mirror cell with active optics support. Axial and lateral support are controlled by separate loops which determine the command signals for the actuators (A)

combining and synchronization [Vilnrotter et al. (2005)]. Furthermore, single apertures outperform arrays under different circumstances, e.g. when background radiation is present.

This paper proposes a system to build lightweight, low-cost telescopes with large aperture in order to solve the problem of large mass and high costs of OGSs with larger aperture and to avoid the drawbacks that come with telescope arrays of smaller apertures. The utilization of an active optics system, first developed for the New Technology Telescope (NTT) of the ESO [Wilson et al. (1987)], for the support structure of the primary mirror allows a large reduction of mirror mass since actuators at the mirror are able to compensate for angle-dependent gravitational deflection of the thinner and more flexible mirror. Additionally, time, energy and cost of mirror production is decreased significantly because of less consumption of expensive low thermal expansion material as well as eased requirements regarding surface shape after polishing. Furthermore, the effort of aligning of the telescope, for instance after transportation or under different environmental circumstances, is greatly decreased since it can use the implemented sensors and actuators to align itself.

The paper is organized as follows: Sec. 2 provides a brief description of the primary mirror system. An optimization of a continuous support based on an analytical model is presented in Sec. 3 and used as initial value for FEA optimization and transition to discrete actuator location in Sec. 4. In Sec. 5 the actuator sensitivity is investigated. Finally, the conclusion is presented in Sec. 6.

2. SYSTEM OVERVIEW PRIMARY MIRROR

Fig. 1 shows the structure of the primary mirror system with active optics, consisting of the mirror cell, the actuators located within the cell structure, and the primary mirror itself. The support system is divided into an axial and a lateral support to regulate the position and shape of the mirror. While a wavefront sensor (WFS) and force sensors at the actuators give feedback about the shape, position sensors are used for controlling mirror position. As a result, the active optics system enables to correct induced misalignments and figure errors due to temperature gradients, gravity and even shape inaccuracies after production.

Table 1. Material parameter of fused silica and mirror data

Parameter	Symbol	Value	Unit
Density	ρ	2.2	$\mathrm{g \cdot cm^{-3}}$
Young's modulus	E	74	GPa
Poisson's ratio	ν	0.17	–
Mass	m	39.865	kg
Outer diameter	D	1.0	m
Hole diameter	d_h	0.28	m
Thickness	h	0.025	m
Radius of curvature	R_C	3.6	m

This paper, however, focuses on the axial support system as a first design step towards the whole support. The mirror for further analysis to obtain the axial active optics system design is considered a monolithic meniscus with an outer diameter of 1 m, based on the larger apertures of existing OGSs, and is made of fused silica which has a very low thermal expansion coefficient along with good thermal and mechanical properties [Ahmad (2017)]. Constant thickness of 25 mm gives the mirror an aspect ratio of 40 and a mass of only 40 kg. The information that

$$m_{\mathrm{tel}} \approx 10 \cdot m_{\mathrm{prim}}, \tag{1}$$

i.e. the mass of the whole telescope is approximately ten times the mass of the primary mirror [Doeberl (2018)], holds out the prospect of building an extremely lightweight telescope in the 1 m class with a target weight of about 500 kg. The material parameter and mirror data used in further analysis are summarized in Table 1.

According to Nelson et al. (1982), the deflection of a circular plate without shear effects is described by

$$\delta_{\mathrm{rms}} = \frac{3zqD^4(1-\nu^2)}{4Eh^3}, \tag{2}$$

where z is a parameter depending on the support design, q the applied force per unit area, D the plate diameter, ν the Poisson's ratio of the material, E is Young's modulus and h the plate thickness. Under self-weight, the deflection therefore varies as

$$\delta_{\mathrm{rms}} \propto \frac{D^4}{h^2}. \tag{3}$$

For mirror comparison, the aspect ratio D/h can be used as criterion [Bely (2003)]. For deflection, however, Equation (3) gives the true flexibility criterion. Table 2 compares the considered monolithic meniscus mirror with primary mirrors used in astronomical telescopes which also apply an active optics system. Although the aspect ratio of 40 is comparable to the ratio of very large and thin mirrors, the value of the flexibility criterion is a factor of 10 to 100 less. As a result, a small number of point supports should be suitable to achieve a minimal self-weight surface deflection. Additionally, with suitable sensors and active supports it fulfills the requirement of robustness and can be built highly autonomously.

Pre-print version of the article: C. Schwaer, A. Sinn, and G. Schitter, "Mechatronic Approach towards Lightweight Mirrors with Active Optics for Telescope Systems", *8th IFAC Symposium on Mechatronic Systems MECHATRONICS 2019*, 2019.
DOI: 10.1016/j.ifacol.2019.11.641

Table 2. Comparison of meniscus mirrors

Telescope (D in m)	D/h	D^4/h^2 (10^3m^2)
Considered mirror (1.0)	40	1.6
SPM (2.1)	8.08	0.29
VST (2.6)	18.57	2.33
NTT (3.5)	14.58	2.6
TNG (3.5)	15.02	2.76
DAG (4.0)	29.63	14.05
SOAR (4.1)	41	28.26
DKIST (4.2)	56	55.32
VISTA (4.2)	24.71	10.77
DCT (4.3)	43	34.19
Gemini (8.0)	40	102.4
VLT (8.2)	46.86	147.63
Subaru (8.2)	41	113.03

3. ANALYTIC SUPPORT OPTIMIZATION

The axial support is designed to support the mirror along the optical axis with the objective to reduce surface deflection. In a first step, the design is obtained by pointing the mirror to zenith, i.e. letting the optical axis and the gravity vector coincide so that the total weight of the mirror is taken by the axial support. The objective is the minimization of RMS surface deflection while the design parameters are the location and number of point supports. Since a diffraction-limited imaging quality of the mirror is not needed, the requirement is a maximal RMS deviation of $\lambda/30$, i.e. 17 nm if green light in the middle of the visible spectrum is considered. Additionally, the Peak-to-Valley (PV) error should not exceed $\lambda/10$ (51 nm).
In the work of Nelson et al. (1982), a circular plate is analysed based on thin plate theory. It is assumed that the deflection of a circular plate on point supports takes the form

$$w(r,\theta) = \sum_{m=0}^{\infty} w_m(r) cos(km\theta), \tag{4}$$

where r, θ is the support location in polar coordinates measured from the origin at the plate's vertex, $\theta = 2j\pi/k, j = 1, ..., k$ and k the number of point supports. The paper concludes, however, that the deflection on discrete support points can be close to the deflection obtained on continuous rings, which requires much less complex calculations, if the support point design is chosen carefully

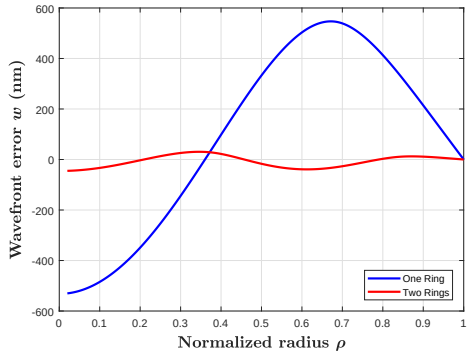

Fig. 2. Deflection of a circular plate under self-weight on one (blue) and two (red) continuous support rings

Table 3. Optimized radii of support rings given by analytical model

	β_1	β_2
One ring	0.686	–
Two rings	0.379	0.842

afterwards [Nelson et al. (1982)]. Therefore, a continuous ring support is considered at first, which simplifies (4) to the first term w_0.
The task at hand is to find the optimal normalized support radius $\beta = r_i/R$, where r_i is the radius of the $i-$th support ring and R is the mirror radius, at which the the RMS deflection of the circular plate is minimal. If the result does not meet the RMS requirement, an additional ring is introduced and the optimization procedere to find the optimal support radii is repeated.
Fig. 2 shows the deflection of the mirror under self-weight on one and two optimized continuous support rings, respectively. As can be seen, the addition of a second ring drastically reduces the deflection. The RMS deviation is decreased from 370 nm to 23.7 nm and the Peak-to-Valley (PV) value from 1077 nm to 75 nm. The optimal normalized radii of the support rings are displayed in Table 3. However, the analytic equations assume a flat circular plate, i.e. an infinite radius of curvature, without a central hole and neglect shear effects. The inclusion of a central hole decreases the weight and area that has to be supported, therefore the two-ring support might already be sufficient to meet the requirement. That is why a finite element analysis (FEA), based on the results of the analytical model, is executed in the next section to account for these effects and further optimize the support.

4. FEM VALIDATION AND OPTIMIZATION

4.1 Mesh

The finite element (FE) mirror model is designed with ANSYS v19.1 and is composed of a structured grid for controlability of node locations and element sizes as well as the reduced computation time. The grid consists of 61440 hexahedrons in 8 layers and has a total number 278160 nodes, whereby the the element size is decreased

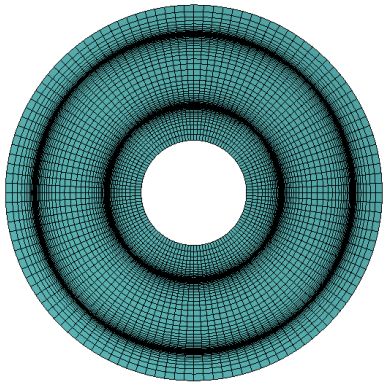

Fig. 3. Front view of the structured mesh showing two support rings

Pre-print version of the article: C. Schwaer, A. Sinn, and G. Schitter, "Mechatronic Approach towards Lightweight Mirrors with Active Optics for Telescope Systems", *8th IFAC Symposium on Mechatronic Systems MECHATRONICS 2019*, 2019.
DOI: 10.1016/j.ifacol.2019.11.641

around the support rings to increase the precision of the analysis. A front view of the grid can be seen in Fig. 3. The coordinate system for the FEA is assumed as follows [Cho (2008)]: the line which connects the primary's to the secondary's mirror vertex corresponds to the Z-axis, the Y-axis equals the mechanical elevation axis of the telescope, the X-axis is defined by the right hand rule and the origin coincides with the mirror vertex.

4.2 Continuous Ring Support

The support radii obtained in Sec. 3 are used as initial value for further FE parameter optimization. The objective is again the minimization of RMS surface deflection. Also, constraints to prevent the mirror from translational x and y and rotational rigid body motion are introduced. The optimization is executed in two processes for reaching the objective. First, a simplified model is used where the support rings are considered as a fixed support in z and the ring radii as design parameter are iteratively adapted. After finding the optimal ring radii in the first step, the fixed support is suppressed and line pressures are applied at the two ring locations which together exactly match the mirror weight. The design parameter in this second step is therefore the weight fraction each support ring takes to achieve the same deflection as on the simplified fixed support. By executing this optimization, the surface deflection of a continuous two-ring support yields a RMS deviation of 8.9 nm and a PV value below 31 nm. The obtained normalized support radii as well as the weight fractions are listed in Tab. 4. Fig. 4 shows the wavefront error over the normalized radius of the mirror with the position of the rings represented by the red vertical lines. Due to the presence of the central hole, the inner support ring can be positioned at a larger radius. The deflection under self-weight meets the requirements well and leaves some margin for the transition to support points, i.e. the number of actuators.

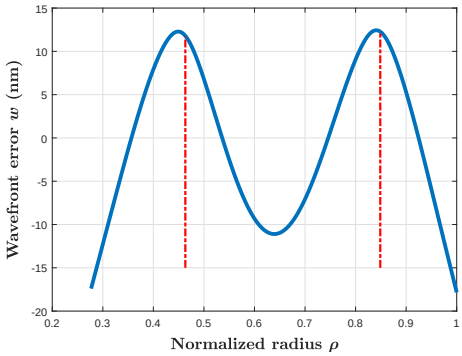

Fig. 4. Deflection of the mirror under self-weight on two continuous support rings (red vertical lines)

Table 4. Normalized radii of support rings

Ring	Norm. Radius	Weight Fraction
1	0.4632	0.3673
2	0.8488	0.6327

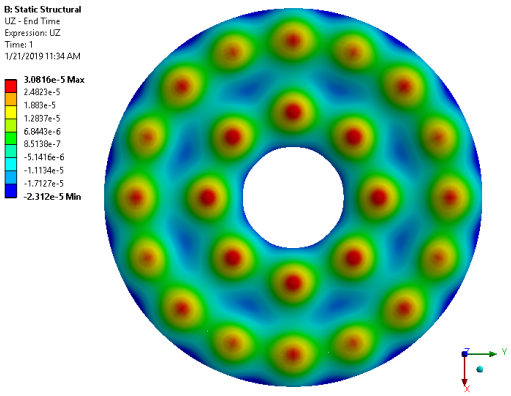

Fig. 5. Surface deflection on a total of 24 axial point supports

4.3 Point Supports

The number of point supports in each ring is chosen such that the azimuthal distance between the supports is less than the radial distance between the rings to limit the deflection degradation caused by the transition from continuous ring support to point supports [Schipani et al. (2010)]. Therefore, the number of supports are chosen to 8 on the first and 16 on the second ring, giving the system a two-fold symmetry. The passive forces acting on the mirror at zenith are derived to $F_{1-8} = 17.95$ N at the inner and $F_{9-24} = 15.46$ N at the outer ring. This axial support design gives a PV error of 54 nm, as shown in Fig. 5, and a RMS error of 10.9 nm. Note that the legend displays the deflection in units of mm. The largest positive deflection is caused by the point support on the inner ring, which could be further reduced by adding more support points, decreasing the force of each support. The largest negative deflection is right at the outer boundary of the mirror halfway between the supports. In summary, with a total of 24 support points for a mirror with a diameter of 1 m and a mass of just below 40 kg, the surface deflection of the optimized design to passively support the mirror successfully meets the requirement of less than 17 nm RMS error and a PV error close to the target specification of 51 nm.

5. ACTIVE SUPPORT SYSTEM

5.1 Elastic modes

It is necessary to investigate the model with respect to its capabilities to actively correct aberrations. This evaluation also gives initial requirements regarding the actuators and sensors that will be used as primary mirror support system. The mirror's elastic modes are the ones which account for most errors after production or during operation, for instance due to unoptimized forces or differences between the support during production and within the mirror cell [Martin et al. (1998)]. The lowest modes are the ones that are most easily excited [Cho (2008)], which is why they can be used to determine the accuracy requirement of the support system.

Pre-print version of the article: C. Schwaer, A. Sinn, and G. Schitter, "Mechatronic Approach towards Lightweight Mirrors with Active Optics for Telescope Systems", *8th IFAC Symposium on Mechatronic Systems MECHATRONICS 2019*, 2019.
DOI: 10.1016/j.ifacol.2019.11.641

Table 5. The first 9 mirror frequency modes

Noll's index	Frequency (Hz)	Mode Shape
5	119.8	Vertical Astigmatism
6	119.8	Oblique astigmatism
9	296.6	Vertical Trefoil
10	296.6	Oblique trefoil
4	299.7	Defocus
7	493.4	Vertical coma
8	493.4	Horizontal coma
14	523.1	Vertical quadrafoil
15	523.1	Oblique quadrafoil

The elastic modes are obtained by using the FE model in modal analysis without any boundary conditions [Cho (2008)]. The first 9 frequency modes, which are the characteristic bending shapes of the mirror, are determined after removing the translational and rotational rigid bode modes. Their frequencies, corresponding Noll's indices and Zernike equivalents are listed in Tab. 5. The low frequency modes do not exactly match the Zernike polynomials, but are very similar to them [Schipani et al. (2010)].

5.2 Support Sensitivity

In order to estimate the required precision with respect to the forces that are applied to the mirror by the supports, a distribution of force errors is chosen to excite astigmatism as the mirror's lowest mode. To this end, a force of 0.1 N is added to the passive forces of four supports on the second ring with an angular spacing of 90° and with alternating signs. With this quite undesirable distribution of force errors the mirror shows astigmatic deflection together with the support's printtrough, see Fig. 6. The radial profile of surface deflection along the x-axis as well as the least-squares fitted parabola representing the Zernike astigmatism are shown in Fig. 7. As can be seen, a force error of only 0.65% with respect to the nominal passive force introduces astigmatism with a RMS error of 23.5 nm. To achieve a surface that is practically free of astigmatic deflection, the support system therefore needs an accuracy of less than 0.1% of the nominal force to be able to actively correct present aberrations.
By using an investigation of the elastic modes of the mirror, a surface deflection is induced by force errors to

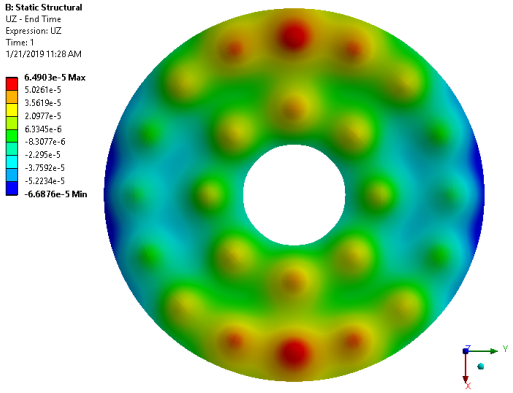

Fig. 6. Astigmatic deflection due to force errors

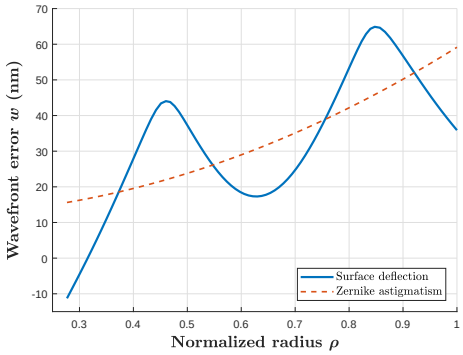

Fig. 7. Profile of the astigmatic deflection in positive x direction due to force errors

successfully determine the accuracy requirement of the support system. In summary, a systematic approach for designing the support of a lightweight mirror is used to obtain the number and location of actuators as well as their requirements. While other 1 m mirrors with active optics use 36 supports [Niu et al. (2012)], the investigation in this paper yields a sufficient surface deflection with 24 actuators and maintains the ability to correct low order aberrations.

6. CONCLUSION

This paper analyzes a thin meniscus mirror in the 1 m class with an aspect ratio of 40 and with 24 actuators supporting the mirror. The actuator location optimization yields a RMS error of 10.9 nm and the lower boundary of the accuracy requirement is obtained to 0.1% of the nominal supporting force. In future work, the analysis will be extended to include the lateral support which takes the arising forces as soon as the optical axis and the gravity vector no longer coincide, which might lead to slight adjustments of the axial support. Furthermore, a system to validate the simulation results will be built.

REFERENCES

Ahmad, A. (2017). *Handbook of Optomechanical Engineering*. CRC Press, Boca Raton, FL, 2nd edition.
Bely, P.Y. (2003). *The Design and Construction of Large Optical Telescopes*. Springer.
Boroson, D.M., Bondurant, R., and Murphy, D.V. (2004). LDORA: a novel laser communications receiver array architecture. In *SPIE Proceedings*, volume 5338.
Cho, M.K. (2008). Performance prediction of the TMT secondary mirror support system. *Proc.SPIE*, 7018.
Doeberl, E. (2018). Telescope mass, ASA Astrosysteme. Private communication.
Garcia-Talavera, M.R., Rodriguez, J.A., Viera, T., Moreno-Arce, H., Rasilla, J.L., Gago, F., Rodriguez, L.F., Gomez, P., and Ramirez, E.B. (2002). Design and performance of the ESA Optical Ground Station. *Proc.SPIE*, 4635.
Hemmati, H., Chen, Y., and Crossfield, I. (2006). Telescope Wavefront Aberration Compensation with a Deformable Mirror in an Adaptive Optics System. *Proc. SPIE*, 6105.

Pre-print version of the article: C. Schwaer, A. Sinn, and G. Schitter, "Mechatronic Approach towards Lightweight Mirrors with Active Optics for Telescope Systems", *8th IFAC Symposium on Mechatronic Systems MECHATRONICS 2019*, 2019.
DOI: 10.1016/j.ifacol.2019.11.641

Kaushal, H. and Kaddoum, G. (2015). Free Space Optical Communication: Challenges and Mitigation Techniques. doi:10.1109/COMST.2016.2603518.

Khalighi, M. and Uysal, M. (2014). Survey on free space optical communication: A communication theory perspective. *IEEE Communications Surveys and Tutorials*, 16(4), 2231–2258.

Kovalik, J.M., Wright, M., Roberts, W.T., and Biswasa, A. (2014). Optical Communications Telescope Laboratory (OCTL) Support of Space to Ground Link Demonstrations. *13th International Conference on Space Operations 2014*, 1–14.

Kudielka, K.H., Kalmar, A., and Leeb, W.R. (1996). Design and breadboarding of a phased telescope array for free-space laser communications. *Proceedings of International Symposium on Phased Array Systems and Technology*.

Leitgeb, E., Awan, M., Brandl, P., Plank, T., Capsoni, C., Nebuloni, R., Javornik, T., Kandus, G., Muhammad, S., Ghassemlooy, F., Loschnigg, M., and Nadeem, F. (2009). Current optical technologies for wireless access. *2009 10th International Conference on Telecommunications*, 7–18.

Link, R., Craddock, M.E., and Alliss, R.J. (2005). Mitigating the impact of clouds on optical communications. *IEEE Aerospace Conference Proceedings*, 2005, 1–8.

Martin, H.M., Callahan, S.P., Cuerden, B., Davison, W.B., DeRigne, S.T., Dettmann, L.R., Parodi, G., Trebisky, T.J., West, S.C., and Williams, J.T. (1998). Active supports and force optimization for the MMT primary mirror. *Astronomical Telescopes & Instrumentation*, 3352, 412–423. doi:10.1117/12.319262.

Nelson, J.R., Lubliner, J., and Mast, T.S. (1982). Telescope Mirror Supports - Plate Deflections on Point Supports. In G. Burbidge and L.D. Barr (eds.), *International Conference on Advanced Technology Optical Telescopes*, volume 332, 212.

Niu, D., Wang, G., and Gu, B. (2012). Active support system for 1-m SONG primary mirror. *Journal of Instrumentation*, 7(5).

Riesing, K., Yoon, H., and Cahoy, K. (2017). A Portable Optical Ground Station for Low-Earth Orbit Satellite Communications. *IEEE International Conference on Space Optical Systems and Applications (ICSOS)*, 108–114.

Riesing, K.M. (2018). *Portable Optical Ground Stations for Satellite Communication*. Ph.D. thesis, Massachusetts Institute of Technology.

Saucke, K., Seiter, C., Heine, F., Gregory, M., Tröndle, D., Fischer, E., Berkefeld, T., Feriencik, M., Feriencik, M., Richter, I., and Meyer, R. (2016). The Tesat transportable adaptive optical ground station. *Proc. SPIE, Free-Space Laser Communication and Atmospheric Propagation*, 9739.

Schipani, P., D'Orsi, S., Ferragina, L., Fierro, D., Marty, L., Molfese, C., and Perrotta, F. (2010). Active optics primary mirror support system for the 2.6m VST telescope. *Appl. Opt.*, 49(8), 1234–1241.

Schulz, K.J., Rush, J., Issler, J.L., Perlot, N., Bertinelli, M., Daddato, R., Montagna, M., Perdigues, J., Popken, L., Sodnik, Z., Van Loock, P., Zayer, I., Inagawa, S., Mukai, T., Park, D.J., Alliss, R., Braatz, L., Cashin, K., Edwards, B., Felton, D., Fletcher, A., Hemmati, H., Jarratt, K., Perko, K., Piazzolla, S., Pollara, F., and Townes, S. (2012). Optical Link Study Group Final Report, Technical Report IOAG.T.OLSG.2012.V1. Technical Report June, Interagency Operations Advisory Group.

Shrestha, A. and Brechtelsbauer, M. (2012). Transportable optical ground station for high-speed free-space laser communication. *Proc SPIE*, 8517.

Toyoshima, M. and Carrasco-Casado, A. (2016). NICT's optical communication projects and ground station development. Presentation at KISS Workshop: Optical Communication on SmallSats.

Toyoshima, M., Takenaka, H., Koyama, Y., Takayama, Y., Kunimori, H., Kubooka, T., Suzuki, K., Yamamoto, S., Taira, S., Tsuji, H., Nakazawa, I., and Akioka, M. (2013). Terrestrial free-space optical communications network for future airborne and satellite-based optical communications projects. *31st AIAA International Communications Satellite Systems Conference, ICSSC 2013*.

Vilnrotter, V., Member, S., Lau, C., Srinivasan, M., Andrews, K., and Mukai, R. (2005). Optical Array Receiver for Communication Through Atmospheric Turbulence. *Journal of Lightwave Technology*, 23(4), 1664–1675.

Wilson, R.N., Franza, F., and Noethe, L. (1987). Active optics I. A system for optimizing the optical quality and reducing the costs of large telescopes. *Journal of Modern Optics*, 34(4), 485–509.

Wojcik, G., Szymczak, H., Alliss, R., Link, R., Craddock, M.E., and Mason, M. (2005). Deep-space to ground laser communications in a cloudy world. *SPIE Proceedings*, 5892.

Pre-print version of the article: C. Schwaer, A. Sinn, and G. Schitter, "Mechatronic Approach towards Lightweight Mirrors with Active Optics for Telescope Systems", *8th IFAC Symposium on Mechatronic Systems MECHATRONICS 2019*, 2019. DOI: 10.1016/j.ifacol.2019.11.641